Astroparticle Physics 30 (2009) 287–292

Contents lists available at ScienceDirect

Astroparticle Physics

journal homepage: www.elsevier.com/locate/astropart

Software timing calibration of the ARGO-YBJ detector

The ARGO-YBJ Collaboration: G. Aielli [a,b], C. Bacci [c,d], B. Bartoli [e,f], P. Bernardini [g,h,*], X.J. Bi [i], C. Bleve [g,h,1], P. Branchini [d], A. Budano [d], S. Bussino [c,d], A.K. Calabrese Melcarne [g,h,2], P. Camarri [a,b], Z. Cao [i], A. Cappa [j,k], R. Cardarelli [b], S. Catalanotti [f,e], C. Cattaneo [l], S. Cavaliere [f,e], P. Celio [c,d], S.Z. Chen [i], N. Cheng [i], P. Creti [h], S.W. Cui [m], G. Cusumano [n,o], B.Z. Dai [p], G. D'Alí Staiti [o,q], Danzengluobu [r], M. Dattoli [j,k,s], I. De Mitri [g,h], B. D'Ettorre Piazzoli [f,e], M. De Vincenzi [c,d], T. Di Girolamo [f,e], X.H. Ding [r], G. Di Sciascio [e,3], C.F. Feng [t], Zhaoyang Feng [i], Zhenyong Feng [u], C. Ferrigno [n,o], F. Galeazzi [d], P. Galeotti [j,s], X.Y. Gao [p], R. Gargana [d], Q.B. Gou [i], H.H. He [i], Haibing Hu [r], Hongbo Hu [i], Q. Huang [u], M. Iacovacci [f,e], I. James [l,v], H.Y. Jia [u], Labaciren [r], H.J. Li [r], J.Y. Li [t], B. Liberti [b], G. Liguori [l,v], C.Q. Liu [p], J. Liu [p], H. Lu [i], G. Mancarella [g,h], S.M. Mari [c,d], G. Marsella [h,w], D. Martello [g,h], S. Mastroianni [c,d], X.R. Meng [r], J. Mu [p], L. Nicastro [o,x], C.C. Ning [r], L. Palummo [a,b], M. Panareo [h,w], L. Perrone [h,w], C. Pino [g,h], P. Pistilli [c,d], X.B. Qu [t], E. Rossi [e], F. Ruggieri [d], L. Saggese [f,e], P. Salvini [l], R. Santonico [a,b], A. Segreto [n,o], P.R. Shen [i], X.D. Sheng [i], F. Shi [i], C. Stanescu [d], A. Surdo [h], Y.H. Tan [i], P. Vallania [j,k], S. Vernetto [j,k], C. Vigorito [j,s], H. Wang [i], Y.G. Wang [i], C.Y. Wu [i], H.R. Wu [i], B. Xu [u], L. Xue [t], H.T. Yang [p], Q.Y. Yang [p], X.C. Yang [p], G.C. Yu [u], A.F. Yuan [r], M. Zha [i], H.M. Zhang [i], J.L. Zhang [i], L. Zhang [p], P. Zhang [p], X.Y. Zhang [t], Y. Zhang [i], Zhaxisangzhu [r], X.X. Zhou [u], F.R. Zhu [i], Q.Q. Zhu [i], G. Zizzi [g,h]

[a] *Dipartimento di Fisica dell'Università "Tor Vergata", via della Ricerca Scientifica 1, 00133 Roma, Italy*
[b] *Istituto Nazionale di Fisica Nucleare, Sezione di Tor Vergata, via della Ricerca Scientifica 1, 00133 Roma, Italy*
[c] *Dipartimento di Fisica dell'Università "Roma Tre", via della Vasca Navale 84, 00146 Roma, Italy*
[d] *Istituto Nazionale di Fisica Nucleare, Sezione di Roma3, via della Vasca Navale 84, 00146 Roma, Italy*
[e] *Istituto Nazionale di Fisica Nucleare, Sezione di Napoli, Complesso Universitario di Monte Sant'Angelo, via Cintia, 80126 Napoli, Italy*
[f] *Dipartimento di Fisica dell'Università di Napoli, Complesso Universitario di Monte Sant'Angelo, via Cintia, 80126 Napoli, Italy*
[g] *Dipartimento di Fisica dell'Università del Salento, via per Arnesano, 73100 Lecce, Italy*
[h] *Istituto Nazionale di Fisica Nucleare, Sezione di Lecce, via per Arnesano, 73100 Lecce, Italy*
[i] *Key Laboratory of Particle Astrophyics, Institute of High Energy Physics, Chinese Academy of Science, P.O. Box 918, 100049 Beijing, PR China*
[j] *Istituto Nazionale di Fisica Nucleare, Sezione di Torino, via P. Giuria 1, 10125 Torino, Italy*
[k] *Istituto di Fisica dello Spazio Interplanetario dell'Istituto Nazionale di Astrofisica, corso Fiume 4, 10133 Torino, Italy*
[l] *Istituto Nazionale di Fisica Nucleare, Sezione di Pavia, via Bassi 6, 27100 Pavia, Italy*
[m] *Hebei Normal University, Shijiazhuang 050016, Hebei, PR China*
[n] *Istituto di Astrofisica Spaziale e Fisica Cosmica di Palermo, Istituto Nazionale di Astrofisica, Via Ugo La Malfa 153, 90146 Palermo, Italy*
[o] *Istituto Nazionale di Fisica Nucleare, Sezione di Catania, Viale A. Doria 6, 95125 Catania, Italy*
[p] *Yunnan University, 2 North Cuihu Rd, 650091 Kunming, Yunnan, PR China*
[q] *Università degli Studi di Palermo, Dipartimento di Fisica e Tecnologie Relative, Viale delle Scienze, Edificio 18, 90128 Palermo, Italy*
[r] *Tibet University, 850000 Lhasa, Xizang, PR China*
[s] *Dipartimento di Fisica Generale dell'Università di Torino, via P. Giuria 1, 10125 Torino, Italy*
[t] *Shandong University, 250100 Jinan, Shandong, PR China*
[u] *South West Jiaotong University, 610031 Chengdu, Sichuan, PR China*
[v] *Dipartimento di Fisica Nucleare e Teorica dell'Università di Pavia, via Bassi 6, 27100 Pavia, Italy*
[w] *Dipartimento di Ingegneria dell'Innovazione, Università del Salento, 73100 Lecce, Italy*
[x] *Istituto di Astrofisica Spaziale e Fisica Cosmica di Bologna, Istituto Nazionale di Astrofisica, Via Gobetti 101, 40129 Bologna, Italy*

* Corresponding author. Address: Dipartimento di Fisica dell'Università del Salento, via per Arnesano, 73100 Lecce, Italy. Tel.: +39 0832 297443; fax: +39 0832 325128.
E-mail address: Paolo.Bernardini@le.infn.it (P. Bernardini).
[1] Present address: School of Physics and Astronomy, University of Leeds, Leeds, United Kingdom.
[2] Present address: INFN-CNAF, Bologna, Italy.
[3] Present address: INFN Sezione di Roma2, Italy.

0927-6505/$ - see front matter
doi:10.1016/j.astropartphys.2008.09.010

ARTICLE INFO

Article history:
Received 23 June 2008
Received in revised form 17 September 2008
Accepted 21 September 2008
Available online 18 October 2008

PACS:
96.50.sd
06.20.Fn
06.30.Ft

Keywords:
Gamma astronomy
Extensive air showers
Timing calibration

ABSTRACT

The ARGO-YBJ experiment is mainly devoted to search for astronomical gamma sources. The arrival direction of air showers is reconstructed thanks to the times measured by the pixels of the detector. Therefore, the timing calibration of the detector pixels is crucial in order to get the best angular resolution and pointing accuracy. Because of the large number of pixels a hardware timing calibration is practically impossible. Therefore an off-line software calibration has been adopted. Here, the details of the procedure and the results are presented.

1. Introduction

The ARGO-YBJ (Astrophysical Radiation Ground-based Observatory at Yang-BaJing) experiment is devoted to VHE γ-astronomy and cosmic ray studies. The detector is located in Tibet (PR China) at an altitude of 4300 m and is a single layer of resistive plate chambers (RPCs) operated in streamer mode. The chambers measure the arrival times of the secondary charged particles, then the primary direction is reconstructed by means of a detailed space-time picture of the air shower. Therefore, the timing calibration of the detector is crucial in order to get the angular resolution and the absolute pointing accuracy required for the astronomy goals. The calibration must remove systematical time offsets among the read-out channels due to differences in the length of the cables, in the discharge time in the chambers, in the electronic circuits and so on.

Due to the large number of pixels (18480 for the whole detector) a hardware timing calibration requires too much time and manpower. Therefore, a software calibration has been adopted. The details of the calibration procedure and its results are presented in this paper.

The correctness of the procedure was confirmed both by a full simulation and by a hardware sampling calibration. The azimuthal distribution after the calibration is coherent with the expectation due to the geomagnetic effect on secondary particles. Finally, also the Moon shadow analysis confirms that the detector is properly calibrated.

2. Detector

The detector setup is shown in Fig. 1. It is essentially a continuous carpet of RPCs on a surface of 78×74 m^2. The fiducial area is enlarged up to 111×99 m^2 by a partially covered guard-ring. The cluster (12 RPCs) is the main DAQ unit, readout by a local station. The RPCs are equipped with pick-up strips (7×62 cm^2) and the fast-OR-signal of 8 strips constitutes the logical pixel (called *pad*) for triggering and timing purposes.

Two different types of data-taking ("scaler" and "shower" mode) are operative. In the first one the coincidence rates are measured on each cluster without any trigger. In "shower mode" a trigger condition is required to collect event data (strip multiplicity and time from the fired pads). In "shower mode" the event is fully reconstructed (core position, shower direction and so on). Since July 2006 the data have been collected with the central carpet (ARGO-130) and the trigger condition $N_{hit} \geqslant 20$, where N_{hit} is the number of fired pads in a time window of 420 ns. In this condition the DAQ rate is $\sim$4 kHz. In 2007 also the guard-ring has been inserted in the DAQ, the rate did not change because the ring hits are not used for trigger purposes.

2.1. Event reconstruction

The event reconstruction is performed by a C++ program (called *Medea++*). Two fit procedures are used in the space-time view in order to determine the arrival direction of the primary rays. They

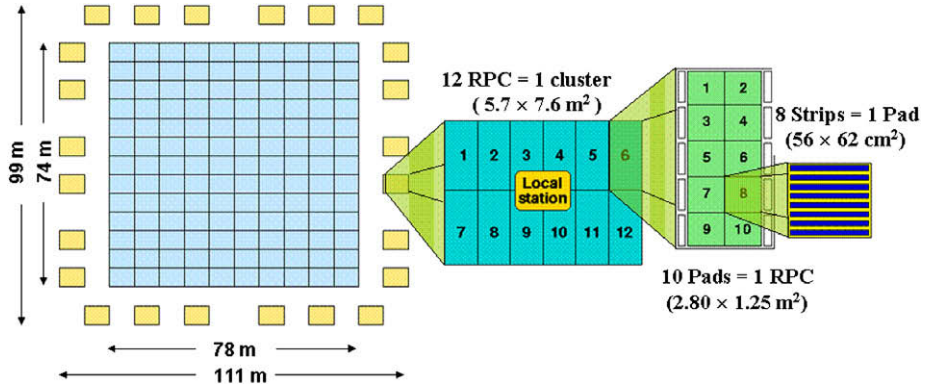

Fig. 1. Detector setup. The cluster (12 RPCs) is the DAQ unit equipped with a local station for the read-out. The full-coverage central carpet is made by 130 clusters, the guard-ring by 24 clusters. The pad (logical-OR of 8 strips) is the timing pixel.

are based on two different assumptions on the shape of the shower front: conical or planar front.

Assuming a conical front of the incoming particles, the arrival times of the particles are fitted by minimizing the following quantity:

$$\chi^2 = \frac{1}{N_{hit}} \sum_{i=1}^{N_{hit}} w_i \left(t_i - t_0 - \frac{l}{c} x_i - \frac{m}{c} y_i - \alpha r_i \right)^2 \quad (1)$$

This quantity is not a standard χ^2 because the time uncertainty is neglected. The reconstructed parameters are the direction cosines l,m and the time t_0, that is the time of the shower plane in the point of coordinates (0,0). The sum is over the fired pads, w_i is the number of strips fired in the ith pad, t_i is the measured time, x_i, y_i are the pad coordinates and c is the light velocity. The conicity correction depends on the conicity coefficient ($\alpha = 0.1$ ns/m) and on the pad distance (r_i) to the core in the shower plane. Some algorithms have been implemented in the *Medea++* code for the determination of the core position. For the calibration procedure the maximum likelihood method has been used assuming that the lateral density distribution is in agreement with a NKG-like function. Removed the conical correction, the Eq. (1) becomes valid in the hypothesis of planar showers (planar fit).

3. Timing calibration

Timing calibration means to estimate the necessary systematical correction of the pad time measurements. We adopted the characteristic plane (CP) method fully described in [1]. This method takes the secondary particles in a shower as the calibration beam, which is quasi-parallel to the primary direction. If the primary directions are known, the detector units can be relatively calibrated with a set of shower events. The primary direction is reconstructed using the space-time information of the detector units fired in a shower. Due to the detector time offsets, there exists a systematic error between the reconstructed primary direction and the true one, which corresponds exactly to the slope of a characteristic plane defined by the time offsets of the detector units fired by the event. Events firing the same units have the same CP, whose direction cosines are exactly the averages of the direction cosines of the event set if the shower azimuth is uniformly distributed. In practice, the CP is estimated by the average over the whole event set. The reconstructed directions of the events are then corrected accordingly and used to calculate the detector time offsets. Finally, the time offset of each detector unit is averaged over the whole event set.

The azimuth distribution is generally not uniform in most EAS arrays, e.g. the geomagnetic field causes the asymmetry of the efficiency along the azimuth angle and introduces quasi-sinusoidal modulation to the azimuth distribution. This is taken into account in the CP method. Indeed the time offsets by the CP method contains the effect of this pre-modulation. The remnant modulation of the azimuth distribution allows to estimate the pre-modulation, and the time calibration can be corrected accordingly if needed.

The calibration procedure is iterated, i.e. the resulting time offsets are removed from the TDC times in the next iteration, thus the reconstructed directions gradually approach the true ones and the time offsets decrease. The iteration finishes when the differences of the time offsets between two steps are small enough. Generally, the iteration converges after several steps. Anyway the whole procedure is very fast.

Events with large number of hits sample almost all parts of the array thus they have approximately the same CP which corresponds to that of the whole carpet. Indeed for the ARGO-YBJ experiment, events with more than 1500 hits (nearly 10% of all the pads are fired) and with the reconstructed core located inside the central carpet are selected for calibration purposes. The above criteria promise:

- The CPs of the single events are a good estimate of the CP of the whole carpet.
- Good angular resolution and reliable reconstruction of the core in order to improve the estimate of the direction of the calibration beam.
- The parameter α used for the conical correction is well suited (the collimation of the calibration beam is under control).
- Minor geomagnetic effect on the azimuth distribution which can be corrected with high accuracy or is even negligible.

Obviously the timing calibration is valid for all the events, not only for those used in the CP procedure.

3.1. Operative procedure, data sample and event selection

The effective goal of the CP procedure is to push to about 0 the mean values of fit residuals and direction cosines. The first step is the estimate of the mean values of the direction cosines. These mean values fix the CP in the space ct,x and y according to the equation

$$\langle l \rangle x + \langle m \rangle y - ct^{CP} = 0 \quad (2)$$

Then, the fit residuals are estimated with respect to the CP. For a generic event the CP residual of the ith fired pad is

$$\begin{aligned} \delta_i &= t_i - \left(t_i^{fit} - t_i^{CP} \right) \\ &= t_i - \left[(l - \langle l \rangle) \frac{x_i}{c} + (m - \langle m \rangle) \frac{y_i}{c} + \alpha r_i + t_0 \right] \end{aligned} \quad (3)$$

where t_0 is the same for all the pads and is negligible for the timing calibration purposes. For each pad the calibration correction is the median value of δ_i estimated on the full calibration sample. The procedure is repeated, at each step the new time corrections are added to the previous ones. Typically, before six repetitions the new corrections become negligible and the procedure is stopped. The correction suggested by the remnant modulation of the azimuth distribution is negligible, therefore it is not applied.

The modularity of the array allowed to take data during the detector construction. The calibration has been applied to different detector setups with different numbers of clusters in data-taking (ARGO-42, ARGO-104, ARGO-130 and ARGO-154 with the guard-ring). Dedicated data-taking is not necessary, then standard data have been used requiring only that all the operative clusters are in data-taking and the detector performance is stable. This paper is mainly based on the results of ARGO-130 calibration.

The events used for the calibration are selected according to the criteria presented before. That is events whit the core position reconstructed inside the central carpet and with more than 1500 hits (500 hits for ARGO-42, 1000 hits for ARGO-104). As an effect of these cuts, about 1.5 days of data-taking are necessary in order to collect the calibration data set. The size of the sample has been determined in order to make lower than 0.05 ns the uncertainty on the median value of the residual distribution of each pad (more than 80×10^3 hits for each pad). As an example, the TDC distribution and the residual distribution of a single pad are shown in Fig. 2.

Another calibration operative procedure was tested. Also this procedure was based on the CP method assumptions. In a first step the standard residual corrections were applied twice, in a second step a systematical tilting correction was applied according to the mean values of the direction cosines. The events were selected requiring only that the core was reconstructed on the detector.

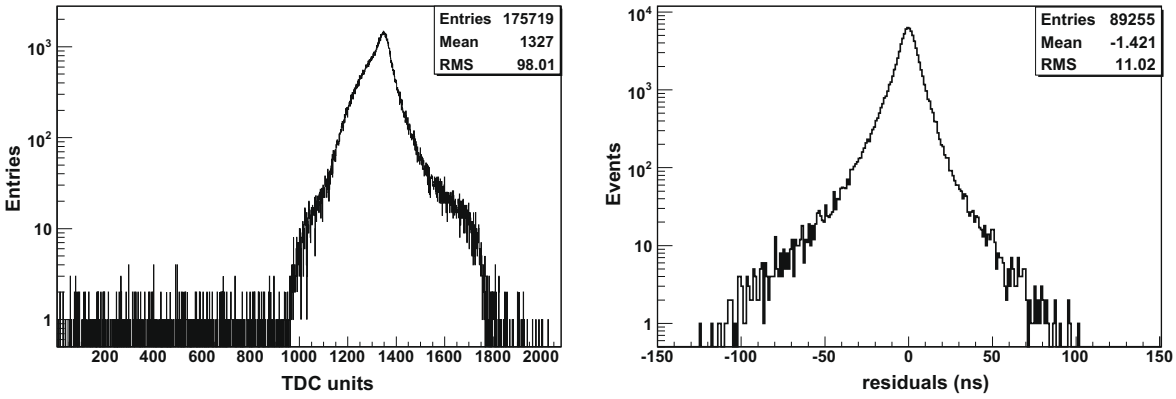

Fig. 2. Examples of TDC (left plot) and conical residual (right plot) distributions for a single pad (pad 120, cluster 88).

This calibration was applied to ARGO-42 data without significant differences with respect to the results of the calibration procedure presented before.

3.2. Calibration results

The comparison between some quantities before and after timing calibration are shown in Figs. 3–5 and Table 1. As expected the mean residual distribution is strongly reduced and the new distribution is a Gaussian with negligible standard deviation (right plot of Fig. 3). The mean residual map is almost uniform (right plot of Fig. 4) with a slight circular structure due to the fact that the shape of the showers is not fully reproduced by the conical fit. The mean values of the direction cosines become fully compatible with zero (Table 1), the azimuth distribution becomes almost flat as expected for an isotropic cosmic ray flux (right plot of Fig. 5). The small modulation visible in the calibrated azimuthal distribution is due to the geomagnetic field and will be discussed in Section 5.

As an effect of the residual reduction, also the χ^2 quantity (Eq. (1)) is smaller. The chess-board method [2] has been used to check

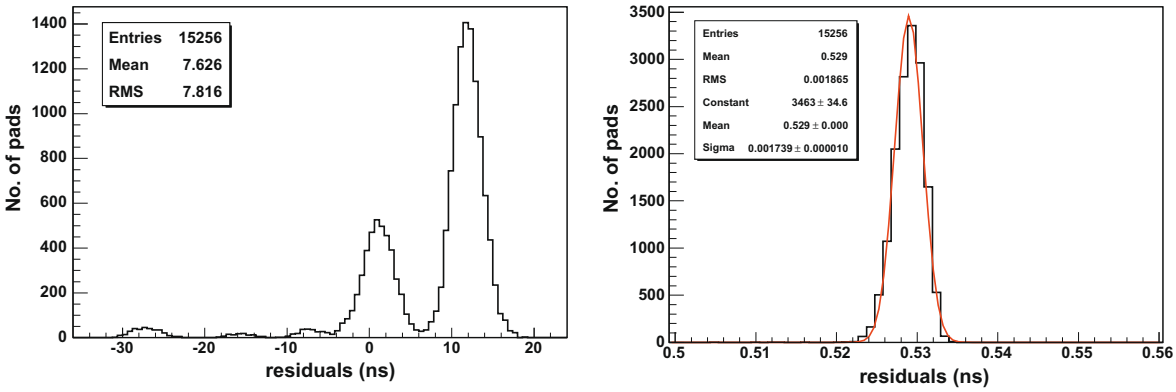

Fig. 3. Conical mean residual distribution before (left plot) and after (right plot) the calibration. A small amount of pads (2.2%) is off. The Gaussian fit is superimposed on the right distribution.

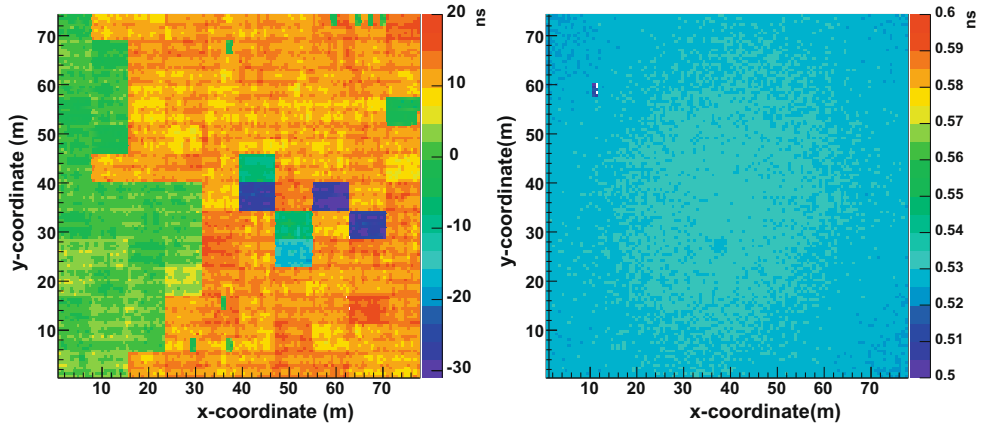

Fig. 4. Conical mean residual vs pad position before (left plot) and after (right plot) the calibration. A small amount of pads (2.2%) is off.

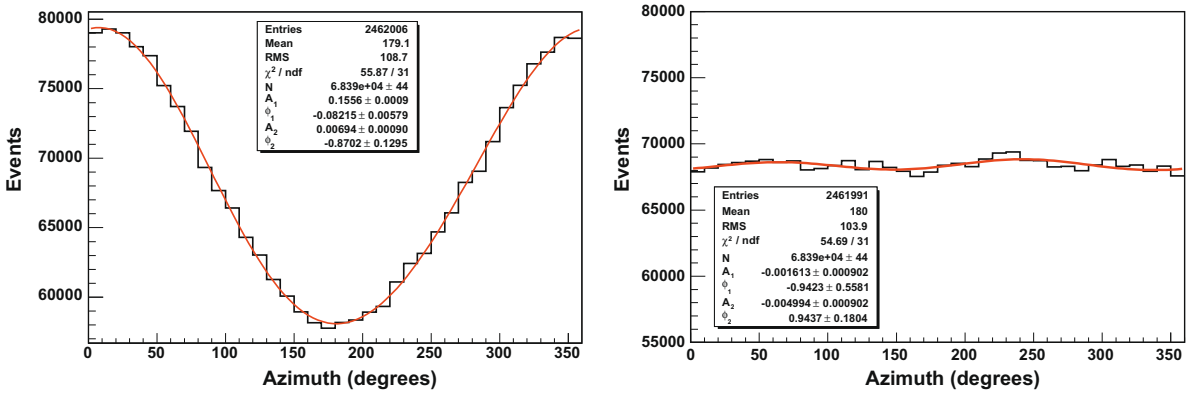

Fig. 5. Azimuth distribution before (left plot) and after (right plot) the calibration. The fit with the two-harmonics function (4) is superimposed.

Table 1
Values of some reconstruction parameters before and after the calibration procedure. The odd-even ψ_{72} value [2] has been estimated for events with more than 100 fired pads.

	Before calibration	After calibration
Residual mean value (ns)	7.626	0.529
Residual RMS (ns)	7.816	0.002
Mean direction cosine m ($\times 10^{-4}$)	455.3 ± 0.2	-0.2 ± 0.2
Mean direction cosine l ($\times 10^{-4}$)	42.7 ± 0.2	0.0 ± 0.2
Mean χ^2 for conical fit of the showers (ns^2)	122.4	79.0
Fit of the ϕ distribution:		
- first harmonics coefficient (A_1)	0.1556 ± 0.0009	0.0016 ± 0.0009
- second harmonics coefficient (A_2)	0.0069 ± 0.0009	0.0050 ± 0.0009
Mean θ value (degrees)	24.570 ± 0.007	24.452 ± 0.007
ψ_{72} for odd-even analysis (degrees)	3.5	2.8

the angular resolution of the detector and will be argument of a future paper. Here, we like to stress the strong reduction of the angular difference (ψ_{72} in Table 1) between the direction reconstructed with the odd pads and that reconstructed with the even pads. Finally, in Table 1 we observe also the slight reduction of the zenith (θ) mean value, explained and foreseen in [3].

4. Check with the hardware calibration

A hardware calibration has been applied to check the software calibration. Two hundred forty pads sampled uniformly among the carpet were manually calibrated using a probe detector. The accuracy of the manual calibration was better than 0.1 ns. During the manual calibration, the DAQ was running normally and the acquired data were used to calibrate the whole carpet using the CP method. The time corrections of these 240 pads by the CP method were compared with those by the manual calibration. The differences are shown in Fig. 6. The mean value of the distribution is meaningless, while the width of 0.45 ns shows the CP method is accurate enough for the ARGO-YBJ experiment.

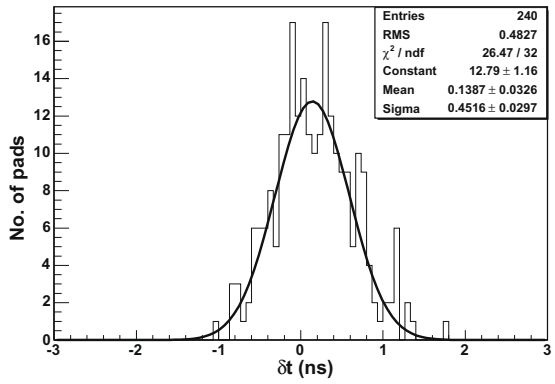

Fig. 6. Comparison between hardware and software calibration for 240 pads. A Gaussian fit is superimposed.

5. Geomagnetic modulation

The geomagnetic cutoff rigidity at the YBJ site (latitude 30° 06′ 38″ N) is estimated to be in the range 11–19 GV depending on the arrival direction [4].

Therefore, the geomagnetic effect on primaries is negligible for events collected in shower mode (the energy threshold is higher than some hundreds of GeV). An effect is expected on secondary particles in the shower [5,6]. This effect must be visible as a small modulation (~1%) of the azimuth (ϕ) distribution, according to the following two-harmonics function:

$$\frac{dN}{d\phi} = K[1 + A_1 cos(\phi - \phi_1) + A_2 cos(2\phi - \phi_2)] \quad (4)$$

A larger modulation is visible in the angular distribution before the calibration (left plot of Fig. 5). Indeed the reconstructed azimuth angles are shifted because the showers are reconstructed with respect to the characteristic plane [1]. This modulation almost disappears after the calibration (right plot of Fig. 5) because the showers are correctly reconstructed with respect to the horizontal plane. According to the CP method a new systematical correction is needed in order to carry back the modulation to the values expected because of the geomagnetic field. Anyway the new correction is so small that we did not apply it. Indeed the parameters (A_1, A_2) of the remnant modulation are already compatible with what expected.

6. Simulation check

A simulation has been used in order to test the efficiency of the CP calibration procedure. The time measurements by each pad have been shifted of an offset. In order to be close to the experimental conditions the real estimated offsets (left plot of Fig. 3) for the data of July 2006 have been used. Four millions of proton-initiated showers have been simulated with Corsika [7]. Their energy is in the range 100 GeV–100 TeV and the arrival zenith angle is lower than 15°. The showers were projected on an area ranging from 200×200 m^2 to 500×500 m^2 proportionally to the

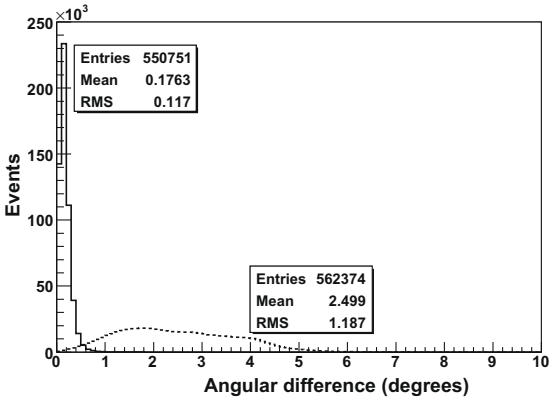

Fig. 7. Data simulated with the trigger real condition ($N_{hit} \geqslant 20$). Hatched histogram: angular differences between the directions reconstructed with the perfect detector (no time offsets) and with the non-calibrated detector (time offsets introduced). Continuous histogram: angular difference between the directions reconstructed with the perfect detector and with the calibrated detector (time offsets and time corrections).

energy. The response of ARGO-130 was reproduced with a Geant-based code (Argog). The simulated data were analyzed in the standard analysis chain by means of the *Medea++* program. The CP calibration was performed analyzing two different data samples: the first one requiring $N_{hit} > 1500$ (standard procedure) and the second one with only the trigger requirement ($N_{hit} \geqslant 20$). When the calibration is derived from events of the second sample the geomagnetic pre-modulation must be taken into account (see [1] for details). When the events used for the calibration have more than 1500 hits, higher energies are selected and the pre-modulation correction is not necessary.

In both cases the time corrections reproduce the systematical offsets. The *RMS* of the calibration-offset differences is ∼0.12 ns. The improvement in the shower angular reconstruction due to the calibration is shown in Fig. 7 for the sample fulfilling the trigger requirement. The shower directions reconstructed with an uncalibrated detector and with a calibrated one are compared with those reconstructed with a perfect detector (without time offsets). For the uncalibrated detector the mean angular difference is ∼2.5°, for the calibrated detector it becomes ∼0.18°.

Also the circular structure of the mean residuals observed in the real data (right plot of Fig. 4) is reproduced in the simulation after the calibration.

7. Calibration validity

During the setting-up/debugging phase the calibration procedure has been repeated many times to correct the new time offsets introduced by the change of cables and electronics modules. Presently the detector is in long-term DAQ for physics run and the calibration stability is checked looking at the changes of the TDC distributions. The calibration updates are not necessary when the hardware is not modified. Typically, the calibration is valid for 30–40 days. Thanks to the calibration update the mean values of reconstructed quantities (zenith angle, χ^2 and so on) are stable.

8. Conclusions

The timing calibration of the ARGO-YBJ detector has been performed with a software procedure and checked with simulation and hardware measurements. This work has been an occasion to study deeply the detector performance. The quality of the primary direction reconstruction improves as a consequence of the calibration. The effect of the geomagnetic field on secondary particles in the shower has been also taken into account. The Moon shadow analysis [8] and the angular resolution studies [2] confirm the reliability of the procedure and will be topics of future papers.

Acknowledgements

This work is supported in China by NSFC (No. 10120130794), the Chinese Ministry of Science and Technology, the Chinese Academy of Sciences, the Key Laboratory of Particle Astrophysics, CAS, and in Italy by the Istituto Nazionale di Fisica Nucleare (INFN).

References

[1] H.H. He et al., Astroparticle Physics 27 (2007) 528–532. also physics/0701291.
[2] G. Di Sciascio et al., for the ARGO-YBJ Collaboration, in: Proceedings of the 30th ICRC, Merida, 2007, p. 573.
[3] A.M. Elø et al., in: Proceedings of the 26th ICRC, Salt Lake City, vol. 5, 1999, pp. 328–331, 320-323 and 324-327.
[4] M. Storini et al., for the ARGO-YBJ Collaboration, in: Proceedings of the 27th ICRC, Hamburg, vol. 10, 2001, pp. 4106–4109.
[5] A.A. Ivanov et al., JETP Letters 69 (1999) 288–292.
[6] M. Bahmanabadi et al., in: Proceedings of the 27th ICRC, Hamburg, vol. 5, 2001, pp. 586–589.
[7] D. Heck, J. Knapp, J.-N. Capdevielle, G. Schatz, T. Thouw, CORSIKA: a Monte Carlo code to simulate extensive air showers, Forschungszentrum Karlsruhe, Report FZKA 6019, 1998.
[8] B. Wang et al., for the ARGO-YBJ Collaboration, in: Proceedings of the 30th ICRC, Merida, 2007, p. 458.